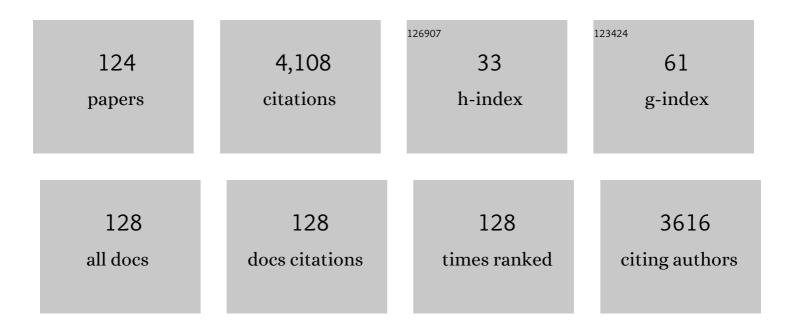
List of Publications by Year in descending order

Source: https://exaly.com/author-pdf/4932122/publications.pdf Version: 2024-02-01



NIDE | FARED

#	Article	IF	CITATIONS
1	Bayesian analysis of depth resolved OCT attenuation coefficients. Scientific Reports, 2021, 11, 2263.	3.3	6
2	Toward improved endoscopic surveillance with multidiameter single fiber reflectance spectroscopy in patients with Barrett's esophagus. Journal of Biophotonics, 2021, 14, e202000351.	2.3	4
3	Experimental validation of a recently developed model for single-fiber reflectance spectroscopy. Journal of Biomedical Optics, 2021, 26, .	2.6	6
4	Effect of probe pressure on skin tissue optical properties measurement using multi-diameter single fiber reflectance spectroscopy. JPhys Photonics, 2020, 2, 034008.	4.6	5
5	Enâ€face optical coherence tomography for the detection of cancer in prostatectomy specimens: Quantitative analysis in 20 patients. Journal of Biophotonics, 2020, 13, e201960105.	2.3	0
6	Subdiffuse scattering model for single fiber reflectance spectroscopy. Journal of Biomedical Optics, 2020, 25, 1.	2.6	10
7	Parametric imaging of attenuation by optical coherence tomography: review of models, methods, and clinical translation. Journal of Biomedical Optics, 2020, 25, 1.	2.6	51
8	Subdiffuse scattering and absorption model for single fiber reflectance spectroscopy. Biomedical Optics Express, 2020, 11, 6620.	2.9	8
9	Analytical model for diffuse reflectance in single fiber reflectance spectroscopy. Optics Letters, 2020, 45, 2078.	3.3	10
10	Noise and bias in optical coherence tomography intensity signal decorrelation. OSA Continuum, 2020, 3, 709.	1.8	12
11	3D co-registration algorithm for catheter-based optical coherence tomography. OSA Continuum, 2020, 3, 2707.	1.8	2
12	Refractive index measurement using single fiber reflectance spectroscopy. Journal of Biophotonics, 2019, 12, e201900019.	2.3	21
13	Grading upper tract urothelial carcinoma with the attenuation coefficient of inâ€vivo optical coherence tomography. Lasers in Surgery and Medicine, 2019, 51, 399-406.	2.1	13
14	Oneâ€ŧoâ€one registration of enâ€face optical coherence tomography attenuation coefficients with histology of a prostatectomy specimen. Journal of Biophotonics, 2019, 12, e201800274.	2.3	10
15	Decreasing the Size of a Spectral Domain Optical Coherence Tomography System With Cascaded Arrayed Waveguide Gratings in a Photonic Integrated Circuit. IEEE Journal of Selected Topics in Quantum Electronics, 2019, 25, 1-9.	2.9	11
16	Multidiameter single-fiber reflectance spectroscopy of heavily pigmented skin: modeling the inhomogeneous distribution of melanin. Journal of Biomedical Optics, 2019, 24, 1.	2.6	9
17	Simple and robust calibration procedure for k-linearization and dispersion compensation in optical coherence tomography. Journal of Biomedical Optics, 2019, 24, 1.	2.6	23

Pathlength distribution of (sub)diffusively reflected light. , 2019, , .

19Needle-based optical coherence tomography for the detection of prostate cancer: a visual and quantitative analysis in 20 patients. Journal of Biomedical Optics, 2018, 23, 1.2.61720Ex-vivo study in nephroureterectomy specimens defining the role of 3-D upper urinary tract visualization using optical coherence tomography and endoluminal ultrasound. Journal of Medical Imaging, 2018, 5, 1.1.5321Spectral domain, common path OCT in a handheld PIC based system. , 2018,	TIONS
<ul> <li>visualization using optical coherence tomography and endoluminal ultrasound. Journal of Medical</li> <li>1.5 3</li> <li>Spectral domain, common path OCT in a handheld PIC based system. , 2018, , .</li> <li>Customized Tool for the Validation of Optical Coherence Tomography in Differentiation of Prostate</li> <li>Cancer. Technology in Cancer Research and Treatment, 2017, 16, 57-65.</li> <li>Noninvasive fluence rate mapping in living tissues using magnetic resonance thermometry. Journal of</li> <li>Biomedical Optics, 2017, 22, 036001.</li> <li>Modeling subdiffusive light scattering by incorporating the tissue phase function and detector numerical aperture. Journal of Biomedical Optics, 2017, 22, 050501.</li> <li>A LED-based phosphorimeter for measurement of microcirculatory oxygen pressure. Journal of Applied</li> <li>Visibility of fiducial markers used for imagea€guided radiation therapy on optical coherence tomography for registration with <scp>CT </scp></li> <li>Visibility of fiducial markers used for imagea€guided radiation therapy on optical coherence tomography for registration with <scp>CT </scp></li> </ul>	
22Customized Tool for the Validation of Optical Coherence Tomography in Differentiation of Prostate Cancer. Technology in Cancer Research and Treatment, 2017, 16, 57-65.1.91323Noninvasive fluence rate mapping in living tissues using magnetic resonance thermometry. Journal of Biomedical Optics, 2017, 22, 036001.2.6324Modeling subdiffusive light scattering by incorporating the tissue phase function and detector numerical aperture. Journal of Biomedical Optics, 2017, 22, 050501.2.61725A LED-based phosphorimeter for measurement of microcirculatory oxygen pressure. Journal of Applied Physiology, 2017, 122, 307-316.2.5426Visibility of fiducial markers used for imagea€guided radiation therapy on optical coherence tomography for registration with <scp>CT</scp> : An esophageal phantom study. Medical Physics, 2017, 3.010	
22       Cancer. Technology in Cancer Research and Treatment, 2017, 16, 57-65.       1.9       13         23       Noninvasive fluence rate mapping in living tissues using magnetic resonance thermometry. Journal of Biomedical Optics, 2017, 22, 036001.       2.6       3         24       Modeling subdiffusive light scattering by incorporating the tissue phase function and detector numerical aperture. Journal of Biomedical Optics, 2017, 22, 050501.       2.6       17         25       A LED-based phosphorimeter for measurement of microcirculatory oxygen pressure. Journal of Applied Physiology, 2017, 122, 307-316.       2.5       4         26       Visibility of fiducial markers used for imageâ€guided radiation therapy on optical coherence tomography for registration with <scp>CT</scp> : An esophageal phantom study. Medical Physics, 2017, 3.0       10	
23       Biomedical Optics, 2017, 22, 036001.       2.0       3         24       Modeling subdiffusive light scattering by incorporating the tissue phase function and detector numerical aperture. Journal of Biomedical Optics, 2017, 22, 050501.       2.6       17         25       A LED-based phosphorimeter for measurement of microcirculatory oxygen pressure. Journal of Applied Physiology, 2017, 122, 307-316.       2.5       4         26       Visibility of fiducial markers used for imageâ€guided radiation therapy on optical coherence tomography for registration with <scp>CT       3.0       10</scp>	
24       numerical aperture. Journal of Biomedical Optics, 2017, 22, 050501.       2.0       17         25       A LED-based phosphorimeter for measurement of microcirculatory oxygen pressure. Journal of Applied       2.5       4         25       Visibility of fiducial markers used for imageâ€guided radiation therapy on optical coherence       2.5       4         26       Visibility of fiducial markers used for imageâ€guided radiation therapy on optical coherence       3.0       10	
<ul> <li>Physiology, 2017, 122, 307-316.</li> <li>Visibility of fiducial markers used for imageâ€guided radiation therapy on optical coherence</li> <li>tomography for registration with <scp>CT</scp>: An esophageal phantom study. Medical Physics, 2017, 3.0 10</li> </ul>	
tomography for registration with <scp>CT</scp> : An esophageal phantom study. Medical Physics, 2017, 3.0 10	
27 OCT Amplitude and Speckle Statistics of Discrete Random Media. Scientific Reports, 2017, 7, 14873. 3.3 34	
Single fiber reflectance spectroscopy calibration. Journal of Biomedical Optics, 2017, 22, 1. 2.6 13	
29 Quantitative attenuation analysis for identification of early Barrett's neoplasia in volumetric laser 2.6 10 endomicroscopy. Journal of Biomedical Optics, 2017, 22, 086001.	
Applicability of quantitative optical imaging techniques for intraoperative perfusion diagnostics: a30comparison of laser speckle contrast imaging, sidestream dark-field microscopy, and optical2.612coherence tomography. Journal of Biomedical Optics, 2017, 22, 1.12	
Assesment of apoptosis induced changes in scattering using optical coherence tomography. Journal of Biophotonics, 2016, 9, 913-923.	
Feedforward operation of a lens setup for large defocus and astigmatism correction. Proceedings of 0.8 1 SPIE, 2016, , .	
Prostate cancer diagnosis by optical coherence tomography: First results from a needle based optical platform for tissue sampling. Journal of Biophotonics, 2016, 9, 490-498.	
Quantitative blood flow velocity imaging using laser speckle flowmetry. Scientific Reports, 2016, 6, 3.3 58 25258.	
Volumetric laser endomicroscopy in Barrett's esophagus: a feasibility study on histological 0.4 22 correlation. Ecological Management and Restoration, 2016, 29, 505-512.	

36 Quantification of numerical aperture-dependence of the OCT attenuation coefficient (Conference) Tj ETQq0 0 0 rgBT /Overlock 10 Tf 50

#	Article	IF	CITATIONS
37	Quantitative Assessment of Optical Properties in Healthy Cartilage and Repair Tissue by Optical Coherence Tomography and Histology. IEEE Journal of Selected Topics in Quantum Electronics, 2016, 22, 203-209.	2.9	1
38	Percutaneous Needle Based Optical Coherence Tomography for the Differentiation of Renal Masses: a Pilot Cohort. Journal of Urology, 2016, 195, 1578-1585.	0.4	15
39	Detection of buried Barrett's glands after radiofrequency ablation with volumetric laser endomicroscopy. Gastrointestinal Endoscopy, 2016, 83, 80-88.	1.0	52
40	The Value of Optical Coherence Tomography in Determining Surgical Margins in Squamous Cell Carcinoma of the Vulva: A Single-Center Prospective Study. International Journal of Gynecological Cancer, 2015, 25, 112-118.	2.5	14
41	<em>In Vivo</em> , Percutaneous, Needle Based, Optical Coherence Tomography of Renal Masses. Journal of Visualized Experiments, 2015, , .	0.3	10
42	Functional optical coherence tomography of pigmented lesions. Journal of the European Academy of Dermatology and Venereology, 2015, 29, 738-744.	2.4	15
43	Prostate cancer diagnosis: the feasibility of needle-based optical coherence tomography. Journal of Medical Imaging, 2015, 2, 037501.	1.5	28
44	Learning curve and interobserver variance in quantification of the optical coherence tomography attenuation coefficient. Journal of Biomedical Optics, 2015, 20, 121313.	2.6	6
45	Validation of quantitative attenuation and backscattering coefficient measurements by optical coherence tomography in the concentration-dependent and multiple scattering regime. Journal of Biomedical Optics, 2015, 20, 121314.	2.6	55
46	Comparison of optical coherence tomography and histopathology in quantitative assessment of goat talus articular cartilage. Monthly Notices of the Royal Astronomical Society: Letters, 2015, 86, 257-263.	3.3	21
47	Spectroscopic Low Coherence Interferometry. , 2015, , 1163-1187.		0
48	Optical density filters modeling media opacities cause decreased SDâ€OCT retinal layer thickness measurements with inter―and intraâ€individual variation. Acta Ophthalmologica, 2015, 93, 355-361.	1.1	18
49	Optical Diagnostics for Upper Urinary Tract Urothelial Cancer: Technology, Thresholds, and Clinical Applications. Journal of Endourology, 2015, 29, 113-123.	2.1	50
50	Optical coherence tomography accurately identifies patients with penile (pre) malignant lesions: A single center prospective study. Urology Annals, 2015, 7, 459.	0.6	6
51	Quantitative comparison of analysis methods for spectroscopic optical coherence tomography: reply to comment. Biomedical Optics Express, 2014, 5, 3034.	2.9	5
52	A literature review and novel theoretical approach on the optical properties of whole blood. Lasers in Medical Science, 2014, 29, 453-479.	2.1	310
53	37 Quantitative Analysis of Volumetric Laser Endomicroscopy Images With Histological Correlation of Ex-Vivo Endoscopic Resection Specimens of Barrett's Esophagus With and Without Early Neoplasia. Gastroenterology, 2014, 146, S-10.	1.3	3
54	Comparison of retinal nerve fiber layer thickness measurements by spectralâ€domain optical coherence tomography systems using a phantom eye model. Journal of Biophotonics, 2013, 6, 314-320.	2.3	19

#	Article	IF	CITATIONS
55	Dependent and multiple scattering in transmission and backscattering optical coherence tomography. Optics Express, 2013, 21, 29145.	3.4	51
56	Volumetric InÂVivo Visualization of Upper Urinary Tract Tumors Using Optical Coherence Tomography: A Pilot Study. Journal of Urology, 2013, 190, 2236-2242.	0.4	66
57	Optical biopsy of epithelial cancers by optical coherence tomography (OCT). Lasers in Medical Science, 2013, 29, 1297-305.	2.1	40
58	Diffuse reflectance relations based on diffusion dipole theory for large absorption and reduced scattering. Journal of Biomedical Optics, 2013, 18, 087007.	2.6	1
59	Quantitative laser speckle flowmetry of the in vivo microcirculation using sidestream dark field microscopy. Biomedical Optics Express, 2013, 4, 2347.	2.9	30
60	Quantitative comparison of analysis methods for spectroscopic optical coherence tomography. Biomedical Optics Express, 2013, 4, 2570.	2.9	33
61	Spectral domain detection in low-coherence spectroscopy. Biomedical Optics Express, 2012, 3, 2263.	2.9	14
62	Optical coherence tomography in vulvar intraepithelial neoplasia. Journal of Biomedical Optics, 2012, 17, 116022.	2.6	35
63	In-situ imaging of articular cartilage of the first carpometacarpal joint using co-registered optical coherence tomography and computed tomography. Journal of Biomedical Optics, 2012, 17, 060501.	2.6	17
64	Functional Optical Biopsy of epithelial tumors. , 2012, , .		0
65	Differentiation between normal renal tissue and renal tumours using functional optical coherence tomography: a phase I <i>in vivo</i> human study. BJU International, 2012, 110, E415-20.	2.5	61
66	Advanced Diagnostics in Renal Mass Using Optical Coherence Tomography: A Preliminary Report. Journal of Endourology, 2011, 25, 311-315.	2.1	43
67	Measurements of wavelength dependent scattering and backscattering coefficients by low-coherence spectroscopy. Journal of Biomedical Optics, 2011, 16, 030503.	2.6	32
68	Determination of the scattering anisotropy with optical coherence tomography. Optics Express, 2011, 19, 6131.	3.4	64
69	Heartbeat-Induced Axial Motion Artifacts in Optical Coherence Tomography Measurements of the Retina. , 2011, 52, 3908.		63
70	Macular pigment optical density measurements: evaluation of a device using heterochromatic flicker photometry. Eye, 2011, 25, 105-112.	2.1	36
71	Integrated system for combined Raman spectroscopy–spectral domain optical coherence tomography. Journal of Biomedical Optics, 2011, 16, 011007.	2.6	51
72	In vivo low-coherence spectroscopic measurements of local hemoglobin absorption spectra in human skin. Journal of Biomedical Optics, 2011, 16, 100504.	2.6	21

#	Article	IF	CITATIONS
73	Structural and biochemical characterization of the rat retina with combined Raman spectroscopy-spectral domain optical coherence tomography (RS-SDOCT). Proceedings of SPIE, 2010, , .	0.8	0
74	Apoptosis- and necrosis-induced changes in light attenuation measured by optical coherence tomography. Lasers in Medical Science, 2010, 25, 259-267.	2.1	58
75	Evaluation of multi-exponential curve fitting analysis of oxygen-quenched phosphorescence decay traces for recovering microvascular oxygen tension histograms. Medical and Biological Engineering and Computing, 2010, 48, 1233-1242.	2.8	14
76	Quantitative measurement of attenuation coefficients of bladder biopsies using optical coherence tomography for grading urothelial carcinoma of the bladder. Journal of Biomedical Optics, 2010, 15, 066013.	2.6	64
77	Optical phantoms of varying geometry based on thin building blocks with controlled optical properties. Journal of Biomedical Optics, 2010, 15, 025001.	2.6	115
78	Quantitative comparison of the OCT imaging depth at 1300 nm and 1600 nm. Biomedical Optics Express, 2010, 1, 176.	2.9	81
79	Multiple and dependent scattering effects in Doppler optical coherence tomography. Optics Express, 2010, 18, 3883.	3.4	54
80	Concentration Dependent Scattering Coefficients of Intralipid Measured with OCT. , 2010, , .		1
81	Measurements of Wavelength Dependent Scattering Coefficients by Low Coherence Spectroscopy. , 2010, , .		0
82	A New Generation of Optical Diagnostics for Bladder Cancer: Technology, Diagnostic Accuracy, and Future Applications. European Urology, 2009, 56, 287-297.	1.9	127
83	Doppler calibration method for Spectral Domain OCT spectrometers. Journal of Biophotonics, 2009, 2, 407-415.	2.3	11
84	Are quantitative attenuation measurements of blood by optical coherence tomography feasible?. Optics Letters, 2009, 34, 1435.	3.3	52
85	Quantitative measurements of absorption spectra in scattering media by low-coherence spectroscopy. Optics Letters, 2009, 34, 3746.	3.3	32
86	Wavelength swept Ti:sapphire laser. Optics Communications, 2008, 281, 4975-4978.	2.1	8
87	Blood oxygen saturation of frozen tissue determined by hyper spectral imaging. Proceedings of SPIE, 2008, , .	0.8	1
88	NAOMI: nanoparticle-assisted optical molecular imaging. , 2007, , .		1
89	Recent developments in optical coherence tomography for imaging the retina. Progress in Retinal and Eye Research, 2007, 26, 57-77.	15.5	304
90	Abnormal arterial flows by a distributed model of the fetal circulation. American Journal of Physiology - Regulatory Integrative and Comparative Physiology, 2006, 291, R1222-R1233.	1.8	39

#	Article	IF	CITATIONS
91	<title>Hematocrit-dependence of the scattering coefficient of blood determined by optical coherence&lt;br&gt;tomography</title> . , 2006, , .		1
92	Temperature-dependent optical properties of individual vascular wall components measured by OCT. , 2006, 6078, 381.		0
93	NAOMI: nanoparticle assisted optical molecular imaging. , 2006, , .		5
94	Colour Oscillations in Arterioarterial Anastomoses Reflect Natural Differences in Donor and Recipient Oxygenation and Hematocrit. Placenta, 2006, 27, 1055-1059.	1.5	3
95	Doppler optical coherence tomography to monitor the effect of photodynamic therapy on tissue morphology and perfusion. Journal of Biomedical Optics, 2006, 11, 044011.	2.6	24
96	Temperature-dependent optical properties of individual vascular wall components measured by optical coherence tomography. Journal of Biomedical Optics, 2006, 11, 041120.	2.6	31
97	Influence of cataract on optical coherence tomography image quality and retinal thickness. British Journal of Ophthalmology, 2006, 90, 1259-1262.	3.9	104
98	Discrimination of atherosclerotic plaque constituents based on local measurements of optical attenuation coefficents by OCT. , 2005, 5686, 426.		1
99	Discrimination of atherosclerotic plaque constituents based on local measurements of optical attenuation coefficients by OCT. , 2005, , .		0
100	Localized measurement of optical attenuation coefficients of atherosclerotic plaque constituents by quantitative optical coherence tomography. IEEE Transactions on Medical Imaging, 2005, 24, 1369-1376.	8.9	141
101	Optical coherence tomography of the Ex-PRESS miniature glaucoma implant. Lasers in Medical Science, 2005, 20, 41-44.	2.1	21
102	Quantitative optical coherence tomography of arterial wall components. Lasers in Medical Science, 2005, 20, 45-51.	2.1	52
103	Darkfield orthogonal polarized spectral imaging for studying endovascular laser-tissue interactions in vivo-a preliminary study. Optics Express, 2005, 13, 702.	3.4	41
104	Toward assessment of blood oxygen saturation by spectroscopic optical coherence tomography. Optics Letters, 2005, 30, 1015.	3.3	129
105	Curve fitting for quantitative measurement of attenuation coefficients from OCT images. , 2005, , .		4
106	Optical Coherence Tomography of the Ex-pressâ,,¢ Miniature Glaucoma Implant. , 2005, , .		0
107	Apoptosis Induces Temporal Increase in Attenuation as Measured by Optical Coherence Tomography. , 2005, , .		0
108	Calculations of scattering by (de-)oxygenated whole blood. , 2004, , .		0

#	Article	IF	CITATIONS
109	Oxygen Saturation-Dependent Absorption and Scattering of Blood. Physical Review Letters, 2004, 93, 028102.	7.8	222
110	Quantitative measurement of attenuation coefficients of weakly scattering media using optical coherence tomography. Optics Express, 2004, 12, 4353.	3.4	271
111	Oxygen saturation dependent absorption and scattering of whole blood. , 2004, , .		3
112	Low Coherence Spectroscopy (LCS) for depth resolved measurements of optical properties in tissue , 2004, , .		0
113	Measurement of the axial point spread function in scattering media using single-mode fiber-based optical coherence tomography. IEEE Journal of Selected Topics in Quantum Electronics, 2003, 9, 227-233.	2.9	129
114	Light absorption of (oxy-)hemoglobin assessed by spectroscopic optical coherence tomography. Optics Letters, 2003, 28, 1436.	3.3	150
115	Oxygen saturation dependent index of refraction of hemoglobin solutions assessed by OCT. , 2003, , .		1
116	Using optical coherence tomography (OCT) for quantitative measurement of attenuation coefficients of the arterial wall. , 2003, 4949, 495.		0
117	Quantitative attenuation measurements with single-mode fiber-based OCT. , 2003, , .		0
118	Comparative OCT imaging of the human esophagus: How well can we localize the muscularis mucosae?. , 2002, 4619, 187.		0
119	Comparative optical coherence tomography imaging of human esophagus: How accurate is localization of the muscularis mucosae?. Gastrointestinal Endoscopy, 2002, 56, 852-857.	1.0	33
120	Comparative optical coherence tomography imaging of human esophagus: How accurate is localization of the muscularis mucosae?. Gastrointestinal Endoscopy, 2002, 56, 852-857.	1.0	34
121	Detection of apoptosis by optical coherence tomography (OCT). , 2001, 4251, 165.		4
122	<title>Changes in optical properties of cells and tissue after induction of apoptosis</title> ., 2001, , .		1
123	<title>Oxygenation measurements with optical coherence tomography</title> . , 2001, , .		0
124	Blood oxygenation measurements with optical coherence tomography. , 2001, , .		1